major problem would be that back electron transfer is usually fast[25] ($\sim 10^{-9}$ s). One would then have to tune the donor acceptor system in such a manner that the back electron transfer takes place in a time longer than $\sim 10^{-5}$ s. This may be achieved by varying the free energy change for the back electron transfer to be in the Marcus inverted regime and by varying the solvent polarity. The time could be made longer also by increasing the physical separation between the donor and the acceptor.

Finally, we note: (1) the net rotational motion would occur in presence of steady light and that the net motion would stop when the light is switched off. (2) Our motor combines the ideas of devices that have already been used in the literature rotaxanes[2] with idea of a ratchet[21–23]. (3) In the earlier motors that have been suggested, it is the site (station) that is excited/reacted, while for our motor, it is the shuttle that is changed externally. (4) Further, all the earlier suggestions have stations that are different while in our model, all the sites are the same and therefore synthesizing the motor should be easier. (5) In our opinion, the suggested change in design, though simple, is the easiest way to get an efficient working molecular motor. (6) The synthesis of the motor poses a challenge, but it should be possible in the near future, given the abilities that organic chemists have attained in synthesizing elegant structures.

1. Sauvage, J. P. (ed.), *Molecular Machines and Motors*, *Structure and Bonding*, Springer Verlag, Berlin, 2001, vol. 99.
2. Balzani, V., Credi, A., Ramyo, F. and Stoddart, J., Artificial molecular machines. *Angew. Chem. Int. Ed.*, 2000, **39**, 3348.
3. Ballardini, R., Balzani, V., Credi, A., Gandolfi, M. T. and Venturi, M., Artificial molecular-level machines: which energy to make them work?. *Acc. Chem. Res.*, 2000, **34**, 445.
4. Bottari, G., Dehez, F., Leigh, D. A., Nash, P. J., Perez, E. M., Wong, J. K. and Zerbetto, F., Entropy-driven translational isomerism: A tristable molecular shuttle. *Angew. Chem. Int. Ed.*, 2003, **42**, 5886.
5. Ashton, P. R. *et al.*, Acid-base controllable molecular shuttles. *J. Am. Chem. Soc.*, 1998, **120**, 11932.
6. Armaroli, N., Balzani, V., Collin, J.-P., Gavina, P., Sauvage, J.-P. and Ventura, B., Rotaxanes incorporating two different coordinating units in their thread: synthesis and electrochemically and photochemically induced molecular motions. *J. Am. Chem. Soc.*, 1999, **121**, 4397.
7. Ashton, P. R. *et al.*, A photochemically-driven molecular-level abacus. *Chem. Eur. J.*, 2000, **6**, 3558.
8. Leigh, D. A., Wong, J. K. Y., Dehez, F. and Zerbetto, F., Unidirectional rotation in a mechanically interlocked molecular rotor. *Nature*, 2003, **424**, 174.
9. Koumura, N., Zijlstra, R. W. J., van Delden, R. A., Harada, B. and Feringa, B. L., Light-driven monodirectional molecular rotor. *Nature*, 1999, **401**, 152.
10. Vale, R. D. and Milligan, R. A., The way things move: looking under the hood of molecular motor proteins. *Science*, 2000, **288**, 88.
11. Keller, D., Bustamante, C. and Oster, G., The physics of molecular motors. *Acc. Chem. Res.*, 2001, **34**, 412.
12. Leigh, D. A., Troisi, A. and Zerbetto, F., Reducing molecular shuttling to a single dimension. *Angew. Chem. Int. Ed.*, 2000, **39**, 350.
13. Ball, P., Natural strategies for the molecular engineer. *Nanotechnology*, 2002, **13**, R15.
14. Das, B. and Sebastian, K. L., Adsorbed hypostrophene: Can it roll on a surface by rearrangement of bonds?. *Chem. Phys. Lett.*, 2000, **330**, 433.
15. Das, B. and Sebastian, K. L., Molecular wheels on surfaces. *Chem. Phys. Lett.*, 2002, **357**, 25.
16. Das, B. and Sebastian, K. L., Through ring umbrella inversion of a molecular rattle. *Chem. Phys. Lett.*, 2002, **365**, 320.
17. Astumian, D., Thermodynamics and kinetics of a Brownian motor. *Science*, 1997, **276**, 917.
18. Bier, M., *Contemp. Phys.*, 1997, **38**, 371.
19. Brouwer, A. M. *et al.*, Photoinduction of fast, reversible translational motion in a hydrogen-bonded molecular shuttle. *Science*, 2001, **291**, 2124.
20. Feynman, R. P., Leighton, R. B. and Sands, M., *The Feynman Lectures on Physics*, Addison-Wesley, London, 1963, vol. 1, chap. 46.
21. Kelly, T. R., Tellitu, I. and Sestelo, J. P., In search of molecular ratchets. *Angew. Chem. Int. Ed.*, 1997, **36**, 1866.
22. Kelly, T. R., Silva, H. D. and Silva, R. A., Unidirectional rotary motion in a molecular system. *Nature*, 1999, **401**, 150.
23. Sebastian, K. L., Molecular ratchets: verifying the principle of detailed balance and the second law of thermodynamics. *Phys. Rev.*, 2000, **61**, 937.
24. Stanier, C., Alderman, S., Claridge, T. and Anderson, H., Unidirectional photoinduced shuttling in a rotaxane with a symmetric stilbene dumbbell. *Angew. Chem. Int. Ed.*, 2002, **41**, 1769.
25. Credi, A., Molecular level machines and logic gates, Ph D thesis, University of Bologna, 1998.

ACKNOWLEDGEMENTS. I thank Prof. A. G. Samuelson for his comments and Dr Bidisa Das for her comments and for help in preparing the manuscript.

Received 23 February 2004; revised accepted 21 May 2004

Effects of erosion on stable thrust wedges: A new perspective in sandbox analogue modelling

K. K. Agarwal* and G. K. Agrawal

Department of Geology, University of Lucknow, Lucknow 226 007, India

Scaled sandbox analogue models have been used to simulate the growth of Coulomb thrust wedges in isotropic cohesionless and anisotropic cohesionless materials. The internal and surface geometry of such wedges is controlled mainly by parameters like the coefficient of basal friction and the physical properties of the deforming materials. The effects of erosion on a stable Coulomb wedge have been studied and are described here. In the experiment carried out for this study, the uppermost 2 cm material of a developed

*For correspondence. (e-mail: kamalagarwal73@hotmail.com)

wedge has been scraped-off, thus reducing the overburden on the wedge. This also changes the surface slope angle of the stable wedge. In order to maintain the critical angle of the wedge (fixed for every combination of deforming material and basal detachment), there is a noticeable renewed internal deformation by reactivation along some older thrust planes as well as some new planes of detachment that also develop on further contraction in an otherwise stable wedge. The wedge once again starts deforming along these thrusts and also grows vertically. This study proposes that the effects of erosion or mass deficiency in a stable wedge under contractional tectonic environment lead to renewed tectonic activity in the orogenic areas. The removal of material in the orogenic areas is caused mainly by natural processes or is enhanced many folds by anthropogenic activities. The experimental results clearly demonstrate that such activities may cause a renewed phase of tectonics in the orogenic areas, which are already subjected to the processes causing severe mass imbalance.

SANDBOX analogue modelling experiments have been used to simulate the growth of thrust wedges in isotropic cohesionless and anisotropic cohesionless materials[1–6]. The overall geometry of these wedges is controlled by a series of thrust faults, which cause small to large amount of crustal shortening. Thus to study these areas, it becomes important to understand the development and evolution of thrust systems. These systems have been studied by a large number of workers all over the world[7–20], through simple experimental work mainly to delineate the thrust geometry.

The sandbox analogue modelling experiments are carried out to evaluate the effects of different parameters that are responsible for the development of the orogen. Here, the effects of only one parameter are highlighted, i.e. the effects of erosion on an already developed and stable wedge. There have been, though, few attempts made by earlier workers[21–25] to understand the effects of such parameters on stable wedges, none of them have used scaled models to document these changes.

The sandbox analogue modelling technique has been successfully employed to show the development of thrust wedges in contractional regime. Scaled sandbox analogue modelling experiments are done using a deforming material enclosed in a box, where deformation is achieved by pushing the sandpack against the backstop. A wedge develops in front of the backstop through detaching the sand pack along successively evolved thrusts in a self-similar manner. The internal deformation stops (in other words, the wedge stops to grow vertically), when it reaches a critical stage (a critical Coulomb wedge)[3,4,6,7].

The experimental apparatus used in the current modelling technique is a glass box with a wooden base plate and two collapsible wooden backstops, with internal dimensions 150 cm × 20 cm × 20 cm. A motor is present on the right-hand side end to pull the basal detachment sheet attached to it through rollers. A slit is present between the base plate and wooden backstop to facilitate the movement of the basal detachment sheet.

Experiments are carried out using layers of coloured, dry, cohesionless quartz sand over thin Mylar film as basal detachment material (μ_b. 0.47) in the deformation apparatus. A sand pack (2.5 cm thick) starts deforming when the basal detachment sheet is pulled with the help of a motor through a roller at a constant displacement rate of about 1 cm min^{-1}. The vertical wooden backstop (on the right-hand side) checks the movement of the sand pack beyond it, and a wedge starts to form in front of it. The model is deformed up to 44% contraction till a critically tapered wedge is formed[7], with no further internal deformation (Figures 1 *a–f* and 2 *a–f*). This experiment shows that the intermediate value of basal friction (μ_b. 0.47) produces a stable critical wedge with taper angles between 6 and 8°, and internal deformation in the wedge is con-

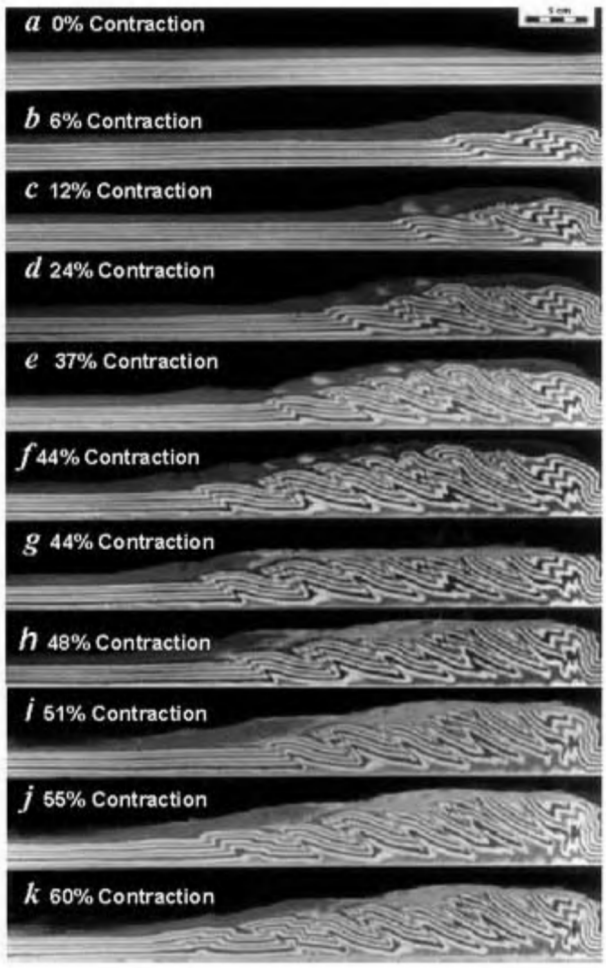

Figure 1. Photographs showing sequential development of wedge in experiment KA-12.

Table 1. Thrust dip angle and wedge taper angle at different stages of shortening

Shortening (%)	Dip of thrust (°)												Wedge taper angle (°)
	Thrust 1	Thrust 2	Thrust 3	Thrust 4	Thrust 5	Thrust 6	Thrust 7	Thrust 8	Thrust 9	Back thrust 1	Back thrust 2	Back thrust 3	
2	28												
12	37	23	35							33			7
24	40	31	34	30	25					35			12
30	46	34	36	35	31	29				34			11
37	50	35	36	35	32	29	31			30			10
43	44	39	38	40	35	35	35	31		35			7
47			40										4
49			40	25						44			5
51			42	26						46			7
55			41	27					26	45	48		8
60			44	29					20	43	53	40	8

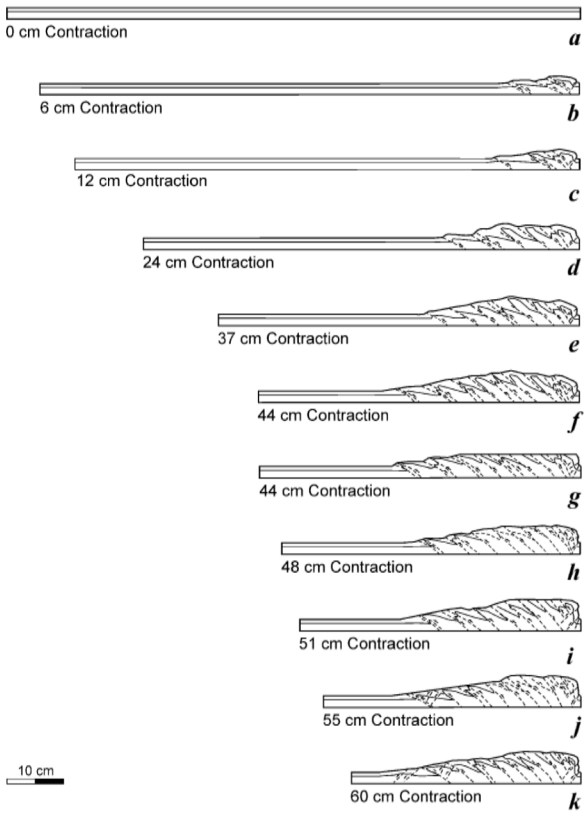

Figure 2. Sequential growth of experiment KA-12, showing successive stages of progressive deformation.

trolled by a series of mainly foreland ward dipping thrusts[7,8,15]. The development of thrusts and their activities up to 44% contraction and beyond are shown in Table 1.

The current analogue experiment is specially planned to observe the effects of erosion on stable wedges. In this experiment, the uppermost material of a developed stable wedge[7] (the height of the wedge at this stage is 6.5 cm) has been scrapped-off by 2 cm (Figures 1 *g–k* and 2 *g–k*), and then the sand pack is again pulled during the experiment. The height of the wedge is now reduced to 4.5 cm by scrapping-off the upper 2 cm material of the wedge (Figures 1 *g* and 2 *g*). The experiment (KA-12) starts after 44% contraction stage on the intermediate basal friction (μ_b. 0.47). At 46% contraction, thrust number three (from the backstop) gets reactivated; hence an increase in the height of the wedge takes place near the backstop (5.4 cm). During the continued deformation, the wedge gets squeezed, and seems to attain more height in order to maintain the critical angle (fixed for every combination of deforming material and basal detachment). At 50% contraction this thrust remains active (Figures 1 *i* and 2 *i*), causing further increase in height (up to 5.8 cm). At next stage of shortening, a splay evolves in the middle of the forethrust, though its effect cannot be seen in the front view. At 52 cm shortening, the length of this active thrust again increases and the height of the wedge becomes 6 cm. The wedge taper angle (Figure 3 *a*) increases from 0 to 6–8° and the thrust angle is 28°. At 53% contraction, a new thrust is developed towards the foreland with an angle of 28°. The displacement along the previously active thrust stops and the movement is now concentrated along this new thrust. At 55% contraction (Figures 1 *j* and 2 *j*), the newly formed forethrust shows the formation of two backthrusts. At 58% contraction, some more features are observed on the surface and it becomes clear at 60 cm contraction that these are two backthrusts at the toe of the wedge. The final wedge taper angle at 60% contraction is 8°. The final wedge taper angle is approximately the same (7°) when the wedge stalls to deform initially at 44% contraction. Afterwards, the wedge stalls and the whole wedge starts sliding over the basal detachment sheet. The central part of the wedge attains a height of 6.4 cm.

The current experiment shows that erosion of material from an already developed wedge has reactivated some of the older thrusts (Figures 1 *g–k*, 2 *g–k* and 3 *b*). This has

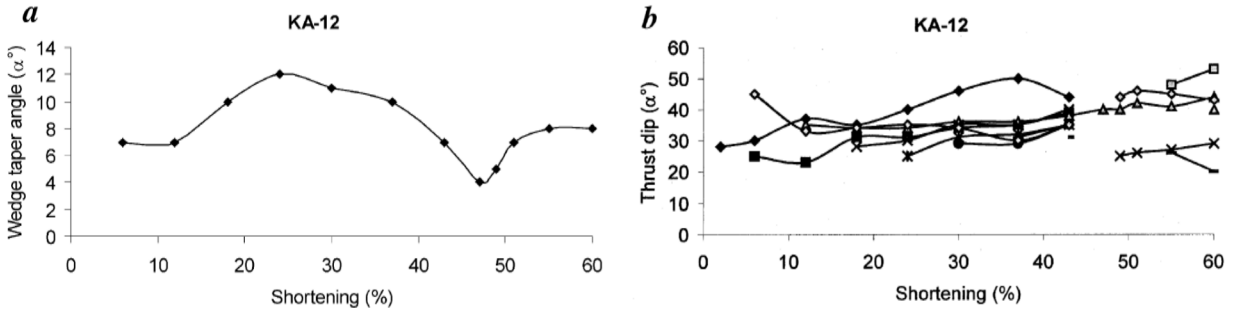

Figure 3. Graph showing progressive changes in (*a*) wedge taper angle vs shortening, and (*b*) thrust dip vs shortening.

been shown in some previous studies also[21,23,25], where the effect of mass transfer from the mountain regions, either due to tectonic instability or climatic changes[21], has renewed tectonic activity in the region. This is mainly because the wedge tends to grow till it attains a critical angle (hence called a critical wedge). The internal deformation ceases when the wedges attain criticality and there is no change in either the thrust geometry or the wedge shape. The moment the critical nature of the wedge is disturbed (by various surface processes), it is again activated in the form of reactivation (Figure 3 *b*) of few older thrusts or by developing newer thrusts in order to maintain the critical character.

Though the physical modelling experiments have many limitations, they still provide a rather simple, graphic and instructive means to explain detailed structural development of thrust systems, which may also be applied to the orogenic belts. The current set of experiments is carried out to study the erosion of material from the stable wedge, which seems to be an important controlling factor on fault reactivation. Erosion, by locally removing sand from the wedge, reduces gravitational and frictional work, enabling continued fault activity or reactivation of older faults. Some new zones of displacement are also formed between the already developed thrusts, i.e. it is not necessary that after erosion only older thrust planes are reactivated; erosion may also lead to the formation of some new thrusts towards the foreland.

1. Boyer, S. E. and Elliott, D., Thrust systems. *AAPG Bull.*, 1982, **66**, 1196–1230.
2. Davis, D., Suppe, J. and Dahlen, F. A., Mechanics of fold-and-thrust belts and accretionary wedges. *J. Geophys. Res.*, 1983, **88**, 1153–1172.
3. Dahlen, F. A., Noncohesive critical Coulomb wedges: an exact solution. *J. Geophys. Res.*, 1984, **89**, 10125–10133.
4. Dahlen, F. A., Critical taper model of fold-thrust belts and accretionary wedges. *Annu. Rev. Earth Planet. Sci.*, 1990, **18**, 55–99.
5. Davis, D. M. and von Huene, R., Inferences on sediment strength and fault friction from structures at the Aleutian Trench. *Geology*, 1987, **15**, 517–522
6. Mitra, G., Evolution of salients in a fold-and-thrust belt: the effects of sedimentary basin geometry, strain distribution and critical taper. In *Evolution of Geological Structures in Macro- to Micro-scales* (ed. Sengupta, S.), Chapman and Hall, London, 1997, pp. 9–90.
7. Agarwal, K. K. and Agrawal, G. K., Sandbox analogue modeling: A useful method to understand evolutionary patterns in different tectonic domains. In *Aspects of Geology and Environment of the Himalaya* (eds Pant, C. C. and Sharma, A. K.), 2002, pp. 159–168.
8. Agarwal, K. K. and Agrawal, G. K., Analogue models of thrust wedges with variable basal frictions. *Gondwana Res.*, 2002, **5**, 641–647.
9. Agarwal, K. K. and Agrawal, G. K., A genetic model of thrust bounded intermontane basin using scaled sandbox analogue models: An example from Karewa basin, Kashmir Himalayas, India. *Int. J. Earth Sci.*, 2004 (communicated).
10. Dahlen, F. A., Suppe, J. and Davis, D. M., Mechanics of fold-and-thrust belts and accretionary wedges: Cohesive Coulomb theory. *J. Geophys. Res.*, 1984, **89**, 10087–10101.
11. Dahlen, F. A. and Barr, T. D., Brittle frictional mountain building, 1, Deformation and mechanical energy budget. *J. Geophys. Res.*, 1989, **94**, 3906–3922.
12. Dahlen, F. A. and Suppe, J., Mechanics, growth, and erosion of mountain belts. In *Processes in Continental Lithospheric Deformation* (eds Clark, Jr. S. P., Burchfiel, B. C. and Suppe, J.), Geol. Soc. Am. Spec. Pap., 1988, vol. 218, pp. 161–178.
13. Bombolakis, E. G., Applicability of critical-wedge theories to foreland belts. *Geology*, 1994, **22**, 535–538.
14. Mandal, N., Chattopadhyay, A. and Bose, S., Imbricate thrust spacing: experimental and theoretical analyses. In *Evolution of Geological Structures in Macro- to Micro-scales* (ed. Sengupta, S.), Chapman and Hall, London, 1997, pp. 143–165.
15. Liu, H., McClay, K. R. and Powell, D., Physical models of thrust wedge. In *Thrust Tectonics* (ed. McClay, K. R.), Chapman and Hall, London, 1992, pp. 71–81.
16. McClay, K. R. (ed.), *Thrust Tectonics*, Chapman and Hall, London, 1992.
17. Mulugeta, G., Modelling the geometry of Coulomb thrust wedges. *J. Struct. Geol.*, 1988, **10**, 847–859.
18. Price, R. A., The mechanical paradox of large overthrusts. *Geol. Soc. Am. Bull.*, 1988, **100**, 1898–1908.
19. Woodward, N. B., Geological applicability of critical-wedge thrust-belt models. *Geol. Soc. Am. Bull.*, 1987, **99**, 827–832.
20. Ziegler, P. A., Van Wees, Jan-Diederik and Cloetingh, S., Mechanical controls on collision-related compressional intraplate deformation. *Tectonophysics*, 1998, **300**, 103–129.
21. Beaumont, C., Fullsack, P. and Hamilton, J., Erosional control of active compressional belt. In *Thrust Tectonics* (ed. McClay, K. R.), Chapman and Hall, London, 1992, pp. 1–18.
22. Gretener, P. E., Pore pressure, discontinuities, isostasy and overthrusts. In *Thrust and Nappe Tectonics* (eds McClay, K. R. and Price, N. J.), Geol. Soc. London Spec. Publ., 1981, vol. 8, pp. 33–39.

23. Huyghe, P., Galy, A., Mugnier, J. L. and France-Lanord, C., Propagation of the thrust system and erosion in the Lesser Himalaya: Geochemical and sedimentological evidence. *Geol. Soc. Am. Bull.*, 2001, **29**, 1007–1010.
24. Lawson, A. C., Isostatic compensation considered as a cause of thrusting. *Geol. Soc. Am. Bull.*, 1922, **33**, 337–351.
25. Moore, G. F., Shipley, T. H. and Lonsdale, P. E., Subduction erosion versus sediment offscraping at the toe of the Middle American Trench off Guatemala. *Tectonics*, 1986, **5**, 513–523.

ACKNOWLEDGEMENTS. We thank Prof. M. P. Singh, Head, Department of Geology, University of Lucknow for providing working facilities and for constant encouragement. We also thank Prof. I. B. Singh for fruitful discussion. This work is part of a DST project awarded to K.K.A. Financial assistance to G.K.A. by CSIR is acknowledged.

Received 8 July 2003; revised accepted 17 March 2004

Development of single-molecule tracking confocal microscope combined with force spectroscopy for gene-expression analysis

Deepak Kumar Sinha[1], Dipanjan Bhattacharya[2], Bidisha Banerjee[1], Feroz Meeran Hameed[1] and G. V. Shivashankar[1,2,*]

[1]National Centre for Biological Sciences, Tata Institute of Fundamental Research, GKVK Campus, Bangalore 560 065, India
[2]Raman Research Institute, C.V. Raman Avenue, Bangalore 560 080, India

We have constructed a confocal fluorescence microscope combined with force measurements. Our method allows for simultaneous measurements of fluorescence anisotropy, energy transfer and correlation. The methodology and the sensitivity of the set-up using enhanced green fluorescent protein are described. We present results on (a) the detection of mRNA polymerization during *in vitro* transcription using fluorescence correlation spectroscopy and anisotropy, (b) detection of *in vivo* protein-DNA interactions using fluorescence anisotropy and (c) nanomanipulation of polytene chromosomes using the micropippete force sensor. Such a combined method allows for probing novel structure–function relationship underlying gene-expression.

RECENT progress in single-molecule force and fluorescence detection[1–3] has opened new possibilities in the area of nanobiology. Typical sensitivity in these measurements is in the range of femtonewton forces[4] and subnanomolar concentrations[3]. The ability to manipulate and detect single-molecules provides a handle to probe the subtle relation among structure, function and dynamics of biomolecules and their interactions. In addition, such methods are finding increasing analytical applications, for example, in sorting and counting of single-molecules, rare-event detection, probe–target binding, high throughput screening, imaging of cells and single-molecule DNA sequencing[5–8]. In the above fluorescence-based studies, a number of specific methods (such as fluorescence correlation spectroscopy (FCS), anisotropy, energy transfer and lifetime techniques) have been used with some advantages and disadvantages. For example, in FCS when analysing heterogeneous molecule ensemble samples, the sampling of multiple events results in ensemble averaging and hence an integrated method using both energy-transfer and anisotropy of molecules would provide a more quantitative method. The intensity and anisotropy recorded at fast binning time (as low as 100 ns) can be used to resolve different conformations and conformational fluctuations of single-molecules. Therefore, a combined experimental set-up that incorporates various fluorescence methods provides a powerful tool to investigate single biomolecular interactions and their dynamics. In addition, its integration to a force sensor allows one to tune the biomolecular structure–function relationship.

Here we describe the development of a confocal fluorescence microscope with fluorescence correlation and anisotropy tracking combined with sensitive micropippete force sensor. We present experiments to address the biophysical aspects of gene-expression that illustrate the importance of the above methods. In particular, we show (a) the detection of mRNA polymerization during *in vitro* transcription using fluorescence anisotropy and correlation spectroscopy, (b) detection of *in vivo* protein–DNA interactions using fluorescence anisotropy and (c) nanomanipulation of polytene chromosomes using the micropipette force sensor.

Figure 1 is a schematic of our experimental set-up. An inverted optical microscope (model IX 70; Olympus, Japan) is placed on a vibration isolation table (model 63–573; Technical Manufacturing Corporation, Peabody, MA, USA). The instrument incorporates an Ar-ion laser (model 163-D0105, 125 mW; Spectra-Physics, Mountain View, CA, USA) for the excitation of the sample. Neutral density (ND) filters (model NDK01; ThorLabs, Newton, NJ, USA) fitted on a filter wheel (model FW2A; ThorLabs) in front of the laser are used to attenuate the power of the laser when so desired. The laser beam diameter is expanded from 0.7 to 4.2 mm using the appropriate lens combination to minimize the focal diameter in the object plane. The beam is passed through a polarizer (model 03 FPG 001, dichroic sheet polarizer; Melles Griot, Rochester, NY, USA) before being passed into the microscope. The laser emits in three wavelengths – 458, 488 and 514 nm. The 488 nm laser line is selected using an excitation filter (model HQ480/40x; Chroma, Brattleboro, VT, USA) fitted in the filter cube (model UMF2; Olympus) of the micro-

*For correspondence. (e-mail: shiva@ncbs.res.in)